Vaccinia Virus Expresses a Novel Profilin with a Higher Affinity for Polyphosphoinositides than Actin†

Laura M. Machesky,‡,§ Nelson B. Cole,‖ Bernard Moss,‖ and Thomas D. Pollard*,‡

Department of Cell Biology and Anatomy, 114 WBSB, The Johns Hopkins University School of Medicine, 725 North Wolfe Street, Baltimore, Maryland 21205, and Laboratory of Viral Diseases, National Institutes of Health, Bethesda, Maryland 20892

Received November 10, 1993; Revised Manuscript Received June 13, 1994®

ABSTRACT: We expressed in *Escherichia coli* the vaccinia virus gene for a protein similar to vertebrate profilins, purified the recombinant viral profilin, and characterized its interactions with actin and polyphosphoinositides. Compared with cellular profilins, this viral profilin has a low affinity ($K_d \geq 35$ μM) for human platelet actin monomers, a weak effect on the exchange of the nucleotide bound to the actin, and no detectable affinity for poly(L-proline). Vaccinia profilin binds to phosphatidylinositol 4,5-bisphosphate and phosphatidylinositol 4-monophosphate in micelles and large unilamellar vesicles, but not to phosphatidylserine or phosphatidylcholine. Kinetic analysis by surface plasmon resonance showed that both vaccinia and amoeba profilins bind slowly to polyphosphoinositides, with association rate constants in the range of (1–4) $\times$ 10^4 M^{-1} s^{-1}. The higher affinity of vaccinia profilin for polyphosphoinositides (K_d = 0.2–8.5 μM) than for actin or poly(L-proline) and the concentration of vaccinia profilin expressed in infected HeLa cells ($\sim$20 μM) suggest that vaccinia profilin binds preferentially to PIP and PIP_2 *in vivo*. Consequently, vaccinia profilin is more likely to influence phosphoinositide metabolism than actin assembly. Expression of 7–105 μM vaccinia profilin in a *Saccharomyces cerevisiae* profilin null mutant did not rescue the null phenotype, so that the affinity of vaccinia profilin for phosphoinositides alone is insufficient for normal profilin function in yeast.

Profilins are highly abundant small proteins required for a normal actin cytoskeleton in both flies (Cooley et al., 1992) and yeast (Haarer et al., 1990). All known cellular profilins bind actin monomers in a 1:1 complex that is incompetent for the spontaneous nucleation of filaments. On the other hand, the profilin–actin complex can elongate the barbed end of actin filaments (Pollard & Cooper, 1984), and profilin may promote the delivery of actin subunits from a pool sequestered by thymosin β_4 to the barbed end of actin filaments (Pantaloni & Carlier, 1993). Profilins also promote exchange of the adenine nucleotide bound to actin (Mockrin & Korn, 1980; Nishida, 1985; Goldschmidt-Clermont et al., 1991b), a process that may contribute to the recycling of actin subunits as actin filaments turn over in cells. Profilins from human platelets (Goldschmidt-Clermont et al., 1990), plants (Drobak, 1993), and *Acanthamoeba* (Machesky et al., 1990) also bind to phosphatidylinositol 4,5-bisphosphate (PIP_2) and inhibit the production of the two important second messengers diacylglycerol and IP_3 by phospholipase C-γ (PLCγ). Phosphorylation of phospholipase C-γ by a receptor tyrosine kinase overcomes this inhibition (Goldschmidt-Clermont et al., 1991a). Actin and PIP_2 compete for binding to profilin (Lassing & Lindberg, 1985, 1988). Thus, profilins are postulated to have a dual role in cells, interacting both with membrane phospholipids to modulate the activities of PLC and with actin monomers to regulate assembly and nucleotide exchange. Activation of the phosphoinositide signalling pathway may be a factor in regulating the cytoplasmic concentration of profilin and thus the interaction of profilin with actin monomers.

Profilin appears to be as ubiquitous as actin, but unlike the highly conserved actin gene family, profilins vary considerably in their primary structures. Sequences are now available from *Drosophila melanogaster* (Cooley et al., 1992), *Saccharomyces cerevisiae* (Oeschner et al., 1987), *Tetrahymena* (Edmatsu et al., 1990), various plants (Valenta et al., 1991, 1992), *Physarum polycephalum* (Takagi et al., 1991), *Dictyostelium discoideum* (Haugwitz et al., 1991), *Acanthamoeba* (Ampe et al., 1985, 1988; Pollard & Rimm, 1990), an echinoderm (Takagi et al., 1991), and vertebrates including human (Kwiatkowski & Bruns, 1988; Honore et al., 1993), mouse (Widada et al., 1989), and cow (Nystrom et al., 1979). Only 18 of 125 residues are conserved among the profilins from vertebrates, *Acanthamoeba*, and yeast. Only nine residues are conserved among all profilins including plants, but comparison of any two profilins (such as human platelet and yeast) yields considerably more sequence identity. In spite of this variation in primary structure, the atomic structures of amoeba (Vinson et al., 1993; Fedorov et al., 1994), bovine (Schutt et al., 1993) and human (Metzler et al., 1993) profilins are very similar. Budding yeast have a single profilin gene, but *Acanthamoeba*, *Dictyostelium*, echinoderms, humans and *Physarum* express more than one profilin from different genes.

Late in infection, vaccinia virus expresses a gene that is 30% identical to mammalian profilin, but the gene is not essential for viral replication in tissue culture (Blasco et al., 1991). During infection with wild-type vaccinia virus, cells

† This work was supported by NIH Research Grant GM-26338 to T.D.P. and by the National Institutes of Health.

* Correspondence should be addressed to this author. Telephone: (410) 955-5664. Fax: (410) 955-4129.

‡ The Johns Hopkins University School of Medicine.

§ Current address: Laboratory of Molecular Biology, Medical Research Council, Hills Rd., Cambridge, England.

‖ National Institutes of Health.

® Abstract published in *Advance ACS Abstracts,* August 1, 1994.

0006-2960/94/0433-10815$04.50/0

round up and cytoplasmic actin bundles enlarge. Virions are associated with actin-containing microvilli through which they are extruded from the cell. Infection of cultured cells with viruses carrying a deletion of the coding region of the profilin gene results in the production of apparently normal virus and the same changes in actin organization detected by immunofluorescence in cells infected with wild-type virus. Possible phenotypes related to the interaction of vaccinia profilin with PIP_2 (such as PI turnover) have not yet been explored.

The biochemical characterization presented in this paper revealed the vaccinia profilin has novel properties compared with other profilins. Purified recombinant vaccinia profilin binds to actin monomers with very low affinity ($K_d \geq 35\ \mu M$) and does not affect actin polymerization *in vitro*, but accelerates the exchange of the nucleotide bound to actin. Unlike any known, naturally occurring profilin, vaccinia profilin does not bind to poly(L-proline). Comparison of the primary structure of vaccinia profilin with the atomic structures of other profilins explains these differences. On the other hand, the affinity of vaccinia profilin for phosphatidylinositol 4-monophosphate (PIP) and PIP_2 is similar to human profilin. These unusual properties suggest that vaccinia profilin may modulate PI turnover during infection, perhaps functioning as an inhibitor of autocrine activation by the EGF-like protein coded by the virus and secreted by infected cells. Expression of vaccinia profilin does not complement a null mutation in the yeast profilin gene, indicating that strong interaction with PIP_2 and PIP is insufficient for the normal function of profilin in these cells.

MATERIALS AND METHODS

Production and Purification of Recombinant Vaccinia Virus Profilin. Construction of an expression plasmid containing the vaccinia virus profilin gene in the pET 3C vector (Rosenberg et al., 1987; Studier et al., 1990) was described previously (Blasco et al., 1991). Cultures of *Escherichia coli (E. coli)* strain BL21 (DE3) containing this construct were started by adding 10 mL of a stationary culture to 1 L of LB medium (Maniatis et al., 1982). All media contained 50 μg/mL carbenicillin and 25 μg/mL chloramphenicol (Sigma, St. Louis, MO). Following incubation for 2 h at 37 °C, expression of vaccinia profilin was induced with 0.4 mM isopropyl β-D-thiogalactopyranoside (BRL, Gaithersburg, MD). After induction, cells grew for approximately 6 h until we harvested them by centrifugation for 30 min at 4 °C at 4000*g*. All subsequent steps were carried out at 0–4 °C. We resuspended the pellets (approximately 2 g of packed cells per liter) (Figure 1, lane 1) in 25 mL of buffer containing chymostatin, leupeptin, antipain, and pepstatin at 50 μg/mL (Sigma), 1 mM phenylmethanesulfonyl fluoride (Sigma), 25 mM Tris-HCl, pH 8, 50 mM sucrose, 1% Triton X-100, 0.5 mM dithiothreitol (DTT), and 0.1 mg/mL lysozyme (Sigma) and lysed the cells by sonication for 5 min on ice with a probe sonicator (Branson-VWR, South Plainsfield, NJ). We centrifuged the homogenate at 150000*g* for 1 h at 4 °C and passed the supernatant (Figure 1, lane 2) through a 2.5 cm × 20 cm column of DEAE-cellulose (Whatman, Maidstone, England) preequilibrated with 50 mM Tris-Cl pH 7.5, 25 mM KCl, 1 mM EDTA, and 0.5 mM DTT. After adding KCl to 100 mM to the flow-through from the DEAE column, we loaded it onto a 2.5 cm × 20 cm column of phosphocellulose (PC; Whatman) equilibrated with PC column buffer (50 mM Tris-HCl, pH 7.5, 100 mM KCl, 1 mM EDTA, and 0.5 mM DTT). The vaccinia profilin eluted from the PC column with a 300 mL linear gradient of 0.05–1 M KCl in 50 mM Tris-HCl, pH 9, 1 mM EDTA, and 0.5 mM DTT. We assayed vaccinia profilin by ELISA using polyclonal antibodies made by injecting rabbits with recombinant vaccinia profilin (Blasco et al., 1991). We dialyzed pooled vaccinia profilin fractions (Figure 1, lane 3) into 25 mM Tris-HCl pH 9, 50 mM KCl, 1 mM EDTA, and 0.5 mM DTT and loaded onto a 2.5 cm × 20 cm hydroxylapatite column (Biorad, Melville, NY) preequilibrated with this buffer. We eluted with a 300 mL linear gradient of 50–500 mM KCl in column buffer and collected 6 mL fractions. We used ELISA to detect fractions containing vaccinia profilin and checked purity by SDS–PAGE (Laemmli, 1970) and staining with Coomassie blue (Figure 1, lane 4). We then incubated pure vaccinia profilin for 2 h at 4 °C with 0.2 g of Bio-beads (Bio-Rad, Richmond, CA), as recommended by the manufacturer, on a tilting agitator to remove any residual Triton X-100. The absorbance at 260 nm decreased by approximately 30% after this incubation, indicating removal of TX-100 from the pure protein. We concentrated protein to approximately 30 μM using Centricon-3 microconcentrators (Amicon, Danvers, MA). We dialyzed protein into hydroxylapatite column buffer at 4 °C and stored it for up to 2 weeks.

Preparation of Other Proteins and Lipids. Rabbit muscle actin was prepared by the method of Spudich and Watt (1971) and gel-filtered on Sephacryl S-300 (2 mM Tris-HCl, pH 7.5, 0.5 mM dithiothreitol, 0.2 mM ATP, 0.1 mM $CaCl_2$, and 0.2 mM NaN_3) to separate monomers from oligomers. Human platelet actin was prepared from outdated platelets (Goldschmidt-Clermont et al., 1991b). Recombinant *Acanthamoeba* profilin-II and recombinant human platelet profilin (Almo et al., 1993; D. A. Kaiser and T. D. Pollard, manuscript in preparation) were prepared from *E. coli* extracts using poly(L-proline) affinity chromatography (Kaiser et al., 1989).

Micelles containing 78 molecules of PIP or PIP_2 (Calbiochem, LaJolla, CA) (Hendrickson, 1969; Sugiura, 1981) or small unilamellar vesicles of phosphatidylcholine (PC; Avanti Polar Lipids, Pelham, AL) and phosphatidylserine (PS; Avanti Polar Lipids) were prepared by drying the lipid under a stream of N_2, dissolving in water by vortexing 1 min, and sonicating in a bath sonicator (Lab Supplies Co., Hicksville, NY) for 3 min. Some vesicles were labeled with trace [^{3}H]PIP_2. Radioactive lipid in chloroform (0.2 μCi = 0.2 nmol from Amersham, Arlington Heights, IL) was dried under a stream of N_2 prior to sonication with PIP_2 in water to form micelles. Large unilamellar vesicles were prepared from these lipid preparations by five freeze–thaw cycles in liquid N_2 and extrusion under high pressure through polycarbonate filters (Hope, 1985) with 0.1 μm pores (Nucleopore, Pleasanton, CA) using an Extruder (Lipex Biomembranes Inc., Vancouver, Canada). These vesicles are about 0.12 μm in diameter (Goldschmidt-Clermont et al., 1990).

Cross-Linking of Vaccinia Virus Profilin to Actin. After dialyzing all proteins separately into 2 mM potassium phosphate, pH 7, for 2 h at 4 °C, we prepared mixtures at final concentrations of 5–10 μM as indicated below in a final volume of 100 or 200 μL. We added 0.2 mg/mL 1-ethyl-3-[3-dimethylamino)propyl]carbodiimide hydrochloride (EDC; Pierce, Rockford, IL) and *N*-hydroxysulfosuccinimide (NHS Pierce, Rockford, IL) for 10 min; then we increased the concentrations of EDC and NHS to 0.4 mg/mL for 20 min, followed by addition of 10 mM glycine in 2 mM potassium phosphate as previously described (Vandekerckhove et al., 1989). SDS–PAGE and Coomassie blue staining allowed visualization of cross-linked species.

Actin Polymerization. We measured actin polymerization by 90° light scattering (Lal & Korn, 1985). Monomeric

human platelet actin (in 10 mM Tris-HCl, pH 7.5, 0.2 mM ATP, and 50 μM dithiothreitol) at a concentration of 4 μM was polymerized by addition of concentrated buffer to final concentrations of 50 mM KCl, 2 mM $MgCl_2$, and 1 mM EGTA. Other samples were tested with human platelet profilin and/or vaccinia virus profilin.

Nucleotide Exchange. We incubated 2 μM human platelet actin in 10 mM Tris-HCl, pH 7.5, 17 μM ATP, 20 μM $CaCl_2$, 0.2 mM EGTA, and 50 μM dithiothreitol containing various concentrations of vaccinia virus profilin at time zero with 167 μM etheno-ATP (1,N^6-ethenoadenosine 5'-triphosphate, Molecular Probes, Eugene, OR) and then measured the fluorescence increase over time (Goldschmidt-Clermont et al., 1991b). We used an excitation wavelength of 360 nm and monitored the fluorescence emission at 410 nm. The exchange data were analyzed by kinetic simulation using KINSIM (Barshop et al., 1983) run on a Macintosh computer (Wachsstock & Pollard, 1994).

Gel Filtration of Vaccinia Profilin and PIP_2. We mixed vaccinia virus profilin with PIP_2 micelles at 22 °C, loaded the mixture on a 0.7 cm × 45 cm column of Sephadex G-100 (Pharmacia, Piscataway, NJ), and collected 0.5 mL fractions. Similar results were obtained with preincubation of column samples for 1 min or 1 h. We used liquid scintillation counting to detect PIP_2 and the Bradford assay (Bio-Rad, Melville, NY) to detect protein. Micelles eluted in the void volume of the column, while profilin was retained in later fractions. We measured the quantity of profilin bound to PIP_2 by subtracting free profilin from total profilin (Machesky et al., 1990).

Measurement of Rate and Equilibrium Constants for Binding of Vaccinia Profilin to Lipids. We measured the rate of binding and dissociation of various lipids to both vaccinia virus and *Acanthamoeba* profilin-II using the BIAcore Biosensor (Pharmacia). We covalently attached vaccinia profilin, *Acanthamoeba* profilin-II, hen egg lysozyme (Sigma) or calf thymus histone type VI-S (Sigma) to separate sensorchips using 0.1 M NHS and 0.4 M EDC to cross-link primary amino groups on the protein to the sensorchip dextran surface (Fagerstam et al., 1992). The sensorchips bound 2.5 ng of vaccinia virus profilin, 17 ng of profilin-II, 2 ng of lysozyme, or 2 ng of histone.

Various lipids in the form of micelles, small unilamellar vesicles, or large unilamellar vesicles were passed over the profilin surfaces to allow binding. The BIAcore biosensor uses surface plasmon resonance (SPR) to measure changes in mass bound to the surface of a sensorchip (Fagerstam et al., 1992). Lipid micelles or large unilamellar vesicles caused an increase in SPR upon interaction with the profilin surface which is measured in resonance units (RU's) approximately equal to 1 pg of mass per RU (Fagerstam et al., 1992). Lipid micelles tested showed no interaction with a surface activated with EDC–NHS in the absence of protein.

Rate and equilibrium constants were determined from single-exponential fits to both association and dissociation data for profilin and lipids using the program "Regression". We selected 100 data points for each fit, usually the first 100 points of any data set, and fit the equation $y = A_0 - A_0 \exp(-kt)$ (association) or $y = A_0 \exp(-kt)$ (dissociation), where y is the binding signal in resonance units (RU's) of SPR, A_0 is the signal in RU's of the maximum binding capacity of the biosensor chip for lipid ligand, t is time in seconds, and k is the variable representing the observed rate constant. We assumed each micelle of 78 lipid molecules bound to 1 profilin. For each combination of lipid and protein, we analyzed the kinetic curves for 4–7 different concentrations of free lipids flowing through the chamber. For the association experiments, we plotted k_{obs} vs the concentration of lipid and obtained k_+ and k_- from the slope and intercept of the linear plots.

Some of the data could not be analyzed quantitatively. A large negative change in the refractive index when large unilamellar vesicles entered the flow cell masked the signal from binding. PS concentrations ≤50 μM gave no signal on the vaccinia profilin chip. At higher concentrations, there was no correlation between lipid concentration and the rate of change of the resonance signal.

Quantitation of Vaccinia Virus Profilin Expression and Endogenous Profilin in Infected HeLa Cells. Confluent monolayers of about 10^6 HeLa cells grown in Dulbecco's modified eagle's medium (Gibco, Grand Island, NY) with 5% fetal calf serum in Costar 12-well culture dishes (Cambridge, MA) were infected with 15 PFU/cell of purified wild-type vaccinia virus strain WR at time 0. At intervals of 2, 4, 6, 8, 12, and 24 h, one dish was lysed in sample buffer (60 mM Tris-HCl, 69 mM SDS, 140 mM β-mercaptoethanol, 109 mM glycerol, and 0.1 mg/mL bromophenol blue) and heated to 95 °C for 10 min. These samples were frozen and stored at −70 °C until use. We electrophoresed samples on a 14% SDS–polyacrylamide gel and blotted the proteins onto nitrocellulose. Vaccinia profilin was detected using a polyclonal rabbit antibody (Blasco et al., 1991) and peroxidase-labeled goat anti-rabbit IgG (Hyclone, Logan, UT). We visualized the profilin bands by chemiluminescence (Amersham) and quantitated the intensity by scanning on an Image Quant (Molecular Dynamics, Sunnyvale, CA). We compared the unknowns with purified vaccinia profilin. Endogenous profilin in HeLa cells was determined in the same manner, using a rabbit anti-human platelet profilin polyclonal antibody, with purified recombinant human platelet profilin as the standard (D. A. Kaiser et al., unpublished results).

Expression of Vaccinia Virus Profilin in Saccharomyces cerevisiae. *S. cerevisiae* strains used were 22ABΔ1-6C *MATa lys2 ura3 his3 trp1 leu2 pfy::LEU2* and 22ABΔ1-6A *MATa lys2 ura3 his3 trp1 leu2* (Haarer et al., 1990).

We constructed a plasmid that would express vaccinia virus profilin in *S. cerevisiae* using YEpIPT, a *TRP1* 2 μm yeast expression plasmid (Hitzeman et al., 1983). After *Eco*RI digestion, we filled in the DNA ends with dNTPs. The linearized plasmid was ligated in the presence of *Bgl*II linkers, creating plasmid YEpA. We inserted a DNA fragment containing the vaccinia profilin coding sequence into this plasmid, creating plasmid YEpVP. Both YEpA and YEpVP were separately transformed into *S. cerevisiae* profilin null mutants (pfy-) (Haarer et al., 1990). Transformants with the *TRP1*-containing plasmids were selected by growth on tryptophan-deficient medium (Sherman et al., 1982).

We prepared cells for SDS–PAGE and blotting onto nitrocellulose (Yaffe & Schatz, 1984) and used the BCA assay (Pierce) to measure protein concentration. Proteins transferred from SDS gels to nitrocellulose were probed with polyclonal anti-vaccinia profilin (Blasco et al., 1991) and visualized using the ECL chemiluminescence system (Amersham). All yeast growth and molecular genetic methods were performed according to standard procedures (Sherman et al., 1982).

RESULTS

Purification of Vaccinia Profilin. Recombinant vaccinia profilin expressed in *E. coli* was soluble after lysis in a sucrose

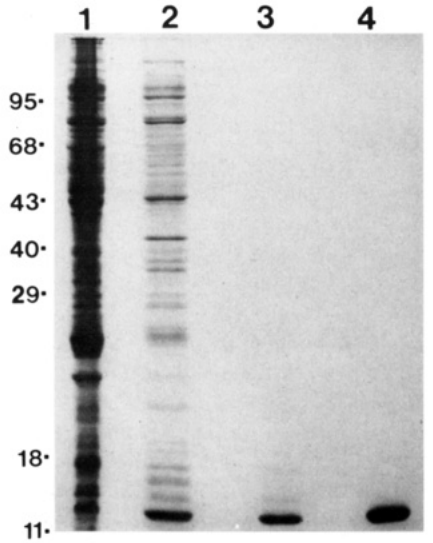

FIGURE 1: Purification of recombinant vaccinia virus profilin. Samples from each step in the purification of recombinant vaccinia virus profilin were separated by SDS–PAGE and stained with Coomassie blue. Lane 1, crude extract of *E. coli* expressing vaccinia profilin; lane 2, supernatant from homogenate; lane 3, elution from phosphocellulose; lane 4, elution from hydroxylapatite.

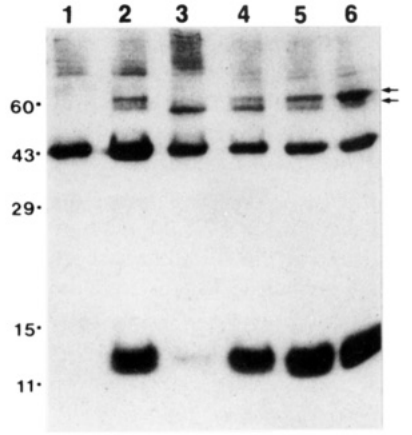

FIGURE 2: Chemical cross-linking of vaccinia profilin to actin. All samples were treated with EDC–NHS prior to being loaded on an SDS gel which was stained with Coomassie blue. Lane 1, 5.3 μM rabbit muscle actin; lane 2, 5.3 μM rabbit muscle actin and 6.5 μM human platelet profilin; lane 3, 5.3 μM rabbit muscle actin and 5.3 μM vaccinia profilin; lane 4, 5.3 μM rabbit muscle actin, 5.3 μM vaccinia profilin, and 5.2 μM human platelet profilin; lane 5, 5.3 μM rabbit muscle actin, 5.3 μM vaccinia profilin, and 10.4 μM human platelet profilin; lane 6, 5.3 μM rabbit muscle actin, 5.3 μM vaccinia profilin, and 18.2 μM human platelet profilin.

and Triton X-100 buffer, so urea denaturation and renaturation used in other profilin purification methods were avoided. We purified vaccinia profilin by ion-exchange chromatography because it did not bind to poly(L-proline)–Sepharose like other profilins. The yield of recombinant vaccinia profilin, which was homogeneous by SDS–PAGE and Coomassie blue staining, was typically 3–4 mg of protein per liter of culture (Figure 1, lane 4). By isoelectric focusing, vaccinia profilin was a single species with pI > 9 (not shown). We stored purified vaccinia profilin in pH 9 Tris-HCl buffer, because it had a tendency to aggregate (detected by 90° light scattering) during storage at pH 7. Vaccinia profilin did not aggregate in 75 mM KCl without buffer over several days at 4 °C, and vaccinia profilin stored in either way eluted from gel filtration columns with the same Stokes radius as other profilins.

Vaccinia Profilin Binds Weakly to Actin Monomers. Treatment of mixtures of vaccinia virus profilin (15 kDa) and rabbit muscle actin (43 kDa) with EDC and NHS produced a protein band on SDS–PAGE of about 55 kDa (Figure 2, lane 3). This band did not appear in samples containing only vaccinia profilin (not shown) or actin alone (Figure 2, lane 1), and it was recognized on immunoblots by the anti-vaccinia profilin polyclonal antiserum. This protein was probably a 1:1 complex of actin and vaccinia profilin. The mobility of the complex of vaccinia profilin and actin on SDS–PAGE was slightly greater than human profilin cross-linked to actin (~58 kDa; Figure 2, lane 2). Human profilin competed with vaccinia profilin for cross-linking to actin (Figure 2 lanes 4–6).

Although vaccinia virus profilin could be cross-linked to actin, it did not inhibit actin polymerization like other profilins at the concentrations tested (Figure 3). While human profilin inhibited the nucleation and elongation phases of spontaneous actin polymerization, even higher concentrations of vaccinia virus profilin did not affect spontaneous polymerization or prevent human profilin from inhibiting spontaneous polymerization (Figure 3).

Vaccinia profilin increased the rate of nucleotide exchange on actin (Figure 4), so we used the concentration dependence of this effect to estimate the equilibrium constant for vaccinia profilin binding to actin. We used the kinetic simulation

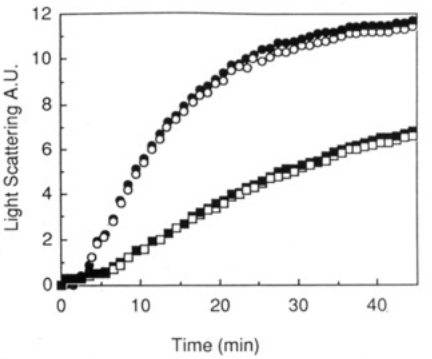

FIGURE 3: Vaccinia virus profilin does not inhibit the spontaneous polymerization of actin. Time course of polymerization is measured by 90° light scattering. Conditions were 10 mM Tris-HCl, pH 7.5, 50 mM KCl, 0.5 mM dithiothreitol, 20 μM ATP, 1 mM EGTA, 2 mM $MgCl_2$, and 4 μM human platelet actin, plus the following concentrations of profilin: 0 μM (○); 8 μM vaccinia profilin (●); 4 μM human profilin (■); 4 μM human profilin + 8 μM vaccinia profilin (□).

program KINSIM (Barshop et al., 1983; Wachsstock & Pollard, 1994) for the analysis. The minimum mechanism has 7 reactions with 14 rate constants (Table 2), but the analysis is tractable because many of the variables are tightly constrained. The association rate constant for etheno-ATP binding to nucleotide-free actin (k_{+2}) is 1 μM^{-1} s^{-1} (Nowak & Goody, 1988). We assume that k_{+1} is the same. The ratio of the dissociation equilibrium constants for etheno-ATP and ATP binding actin is 3 (Pollard et al., 1992). With these constraints, the time course of the exchange of ATP for etheno-ATP on actin alone (Figure 4) gives the absolute values of k_{-1} (0.0013 s^{-1}) and k_{-2} (0.0036 s^{-1}) (Table 2), similar to the values measured under slightly different conditions (Pollard et al., 1992).

For the analysis of reactions involving profilin, we used the reactions listed in Table 2. We assumed that the nucleotides bind to the profilin–actin complex with the same rate constant as for free actin (1 μM^{-1} s^{-1}) and with the same ratio of equilibrium constants (i.e., $3K_d^5 = K_d^6$), but that the rate constants differ for nucleotide dissociation from actin and

Table 1: Rate and Equilibrium Constants for Profilin Binding to Lipids Determined by Surface Plasmon Resonance

immobilized protein	free lipid[a]	data[b]	k_+ (μM^{-1} s^{-1})	k_- (s^{-1})	K_d (μM)
amoeba PII	PIP_2	assoc	0.039	0.056	1.4
amoeba PII	PIP_2	dissoc		0.13	3.3
amoeba PII	PIP	assoc	0.047	0.010	0.2
amoeba PII	PIP	dissoc		0.20	4.3
amoeba PII	PS	assoc	no binding detected		
vaccinia profilin	PIP_2	assoc	0.008	0.066	8.5
vaccinia profilin	PIP_2	dissoc		0.011	1.4
vaccinia profilin	PIP	assoc	0.06	0.042	0.8
vaccinia profilin	PIP	dissoc		0.012	0.2
vaccinia profilin	PS	assoc	binding detected at >50 μM, not analyzable		
vaccinia profilin	PS	dissoc		0.014	
vaccinia profilin	PC/PS	assoc	no binding detected		
vaccinia profilin	PC/PIP_2	assoc	binding detected at >90 μM, not analyzable		

[a] PIP and PIP_2, micellar phosphatidylinositol 4-monophosphate and phosphatidylinositol 4,5-bisphosphate, respectively; PS, small unilamellar vesicles of phosphatidylserine; PC/PS or PC/PIP_2, mixed large unilamellar extruded vesicles of phosphatidylcholine 75% with PS or PIP_2 at 25% by weight. [b] assoc indicates that data from an association reaction were analyzed to calculate the rate constants. dissoc indicates a dissociation experiment.

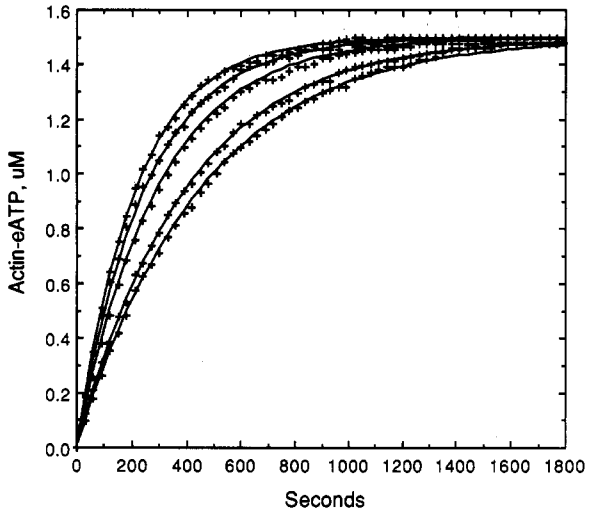

FIGURE 4: Vaccinia virus profilin accelerates the exchange of nucleotide bound to human platelet actin. Conditions were 10 mM Tris-HCl, pH 7.5, 20 μM $CaCl_2$, 17 μM ATP, 0.2 mM EGTA, 2 μM human platelet actin, and various concentrations of vaccinia profilin (curves 1 to 5 numbered from bottom to top): 0 μM (curve 1), 2 μM (curve 2), 8 μM (curve 3), 12 μM (curve 4) or 16 μM (curve 5). The exchange reaction was started by adding 167 μM etheno-ATP. Symbols are data averaged from two separate experiments on different days. The solid lines are theoretical curves obtained by kinetic simulation with the rate constants in Table 2.

Table 2: Kinetic Constants for the Interactions of Actin, Nucleotides, and Vaccinia Profilin

reaction	k_+ (μM^{-1} s^{-1})	k_- (s^{-1})	K_d (μM)
(1) A + T ⇌ AT	1	0.0018	0.0018
(2) A + eT ⇌ AeT	1	0.0054	0.0054
(3) P + AT ⇌ PAT	1	2000	2000
(4) P + AeT ⇌ PAeT	1	2000	2000
(5) PA + T ⇌ PAT	1	0.25	0.25
(6) PA + eT ⇌ PAeT	1	0.75	0.75
(7) P + A ⇌ PA	*a*	*a*	*a*

[a] Reaction 7 is not considered in the simulation.

profilin–actin. We also assumed the rate constant for profilin binding to each actin species (actin, actin–ATP, actin–etheno-ATP) is diffusion-limited with an association rate constant of 1 μM^{-1} s^{-1}. The data do not constrain these rate constants but do constrain the equilibrium constants for these reactions. That is, for a given ratio of rate constants for a reaction, one can vary their values over a wide range without affecting the simulations.

Given the directly measured parameters for reactions 1 and 2 and the foregoing assumptions, the only unknowns are the equilibrium constants for profilin binding to actin–nucleotide (reactions 3 and 4) and for nucleotide binding to profilin–actin (reactions 5 and 6). The relative values of reactions 5 and 6 are fixed at a ratio of 3, so we had only 2 unknowns. The profilin concentration dependence of the time course of nucleotide exchange effectively puts a lower limit on these values. From detailed balance, we know that the binding of nucleotide-free actin to profilin is weak compared with its affinity for ATP. Since the concentration of nucleotide-free actin is low, reaction 7 can be ignored.

The analysis of the time course of nucleotide exchange confirmed that the binding of vaccinia profilin to actin is weak. We searched for combinations of the two unknown constants ($K_d^3 = K_d^4$, $3K_d^5 = K_d^6$; the superscripts indicate the number of the reaction in Table 2) to obtain the best simulations to the four kinetic curves simultaneously. The values for the dissociation of nucleotide from the profilin–actin complex (K_d^5 and K_d^6) must be adjusted in proportion to the equilibrium constants for profilin binding to the actin-nucleotide complex (K_d^3 and K_d^4). For example, if K_d^3 and K_d^4 are 70 μM, K_d^5 is 0.013 μM and K_d^6 is 0.039 μM, meaning that the affinity of profilin–actin for ATP is 7 times weaker than actin for ATP (or ATP dissociates 7 times faster from profilin–actin than from actin). If K_d^3 is 2000 μM, K_d^5 is 0.25 μM, or ATP dissociates 138 times faster than from actin. Over a wide range, the best fit was obtained with a ratio of K_d^5 to K_d^3 of 1.2×10^{-4}. If the value of the dissociation equilibrium constants of ATP from profilin–actin was greater than 35 μM, appropriate values of K_d^5 and K_d^6 gave essentially perfect fits to all four kinetic curves (Figure 4). For values of the dissociation equilibrium constant of profilin from profilin–actin–ATP (K_d^3) less than 35 μM, even the best simulations do not fit the data accurately, because the curves for the low and high concentrations of profilin start to diverge from each other. For example, the mean difference between the half-times of the simulations and the data for the four curves was 19 s for a K_d^3 of 7 μM, 5.5 s for a K_d^3 of 35 μM, 3 s for a K_d^3 of 70 μM, and less than 3 s for K_d^3's of 100–2000 μM. We conclude that K_d^3 is $\geq$35 μM, K_d^4 is $\geq$105 μM, K_d^5 is $\geq$0.008 μM, and K_d^6 is $\geq$0.024 μM. The available data do not place an upper limit on these values, but provide strong evidence that vaccinia virus profilin binds actin much more weakly than other known profilins and that when bound to actin

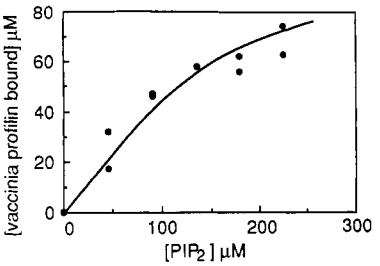

FIGURE 5: Vaccinia profilin binds to micelles of PIP_2. Various concentrations of pure micellar PIP_2 were mixed with 80 μM vaccinia profilin, and the free fraction was measured by small-zone gel filtration. Vaccinia profilin bound to PIP_2 (calculated by subtracting free from total) is shown versus the concentration of PIP_2. The solid line is a theoretical curve calculated using a K_d for vaccinia profilin–PIP_2 of 3.6 μM obtained from kinetic experiments (Table 1) and a stoichiometry of vaccinia profilin–PIP_2 of 1:2.

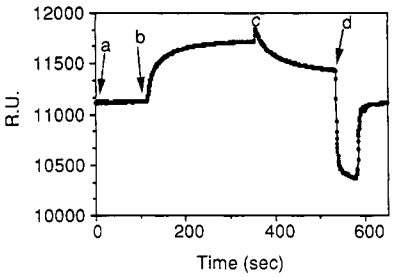

FIGURE 6: Time course of PIP_2 micelle binding to vaccinia virus profilin linked to a BIAcore sensorchip measured in surface plasmon resonance units (RU's). (a) Base line obtained by flowing buffer over the sensorchip. (b) The resonance signal increases as buffer with 50 μM PIP_2 micelles flows across a sensorchip containing covalently linked vaccinia profilin and the lipid interacts with the protein. (c) Buffer alone is flowed across the sensorchip. The resonance signal increases abruptly due to the change in composition (refractive index) and then decreases slowly as lipid micelles dissociate from the profilin surface. (d) The sensorchip is regenerated for the next experiment by washing briefly with 25 mM HCl.

vaccinia profilin lowers the affinity of actin for bound nucleotide modestly.

Vaccinia Profilin Binds to Polyphosphoinositides. We measured the interaction of vaccinia profilin with phospholipids in two ways: small-zone gel filtration (Figure 5) and surface plasmon resonance (Figures 6–8; Table 1). Like other profilins, vaccinia profilin bound to PIP_2 micelles (Figure 5, Table 1), PIP micelles (Table 1), and large unilamellar vesicles of mixed composition containing PIP_2 (Table 1). In small-zone gel filtration experiments, all of the profilin bound when the molar ratio of micellar PIP_2 to vaccinia profilin exceeded 3 (Figure 5). A theoretical binding isotherm calculated with the equilibrium constant derived from the kinetic data in Table 1 fit the equilibrium data in Figure 5. Similar concentrations of phosphatidylserine (PS) or phosphatidylcholine (PC) in small unilamellar vesicles bound little or no vaccinia profilin (not shown).

PIP_2 and PIP micelles bound to vaccinia virus profilin covalently linked to a BIAcore Biosensor chip surface as detected by surface plasmon resonance (Fagerstam et al., 1992). As PIP_2 micelles flowed over the sensorchip, they bound to and saturated the surface that contained covalently linked vaccinia profilin (Figure 6, points b to c). The lipid dissociated from the surface when buffer flowed through the chamber (Figure 6, points c to d). *Acanthamoeba* profilin-II linked to a biosensor chip also bound PIP and PIP_2 (Figure 8B, Table 1). The binding of PIP_2 to the two profilins had a hyperbolic concentration dependence (Figure 7A). PIP_2 interacted weakly with lysozyme, but the binding curves were

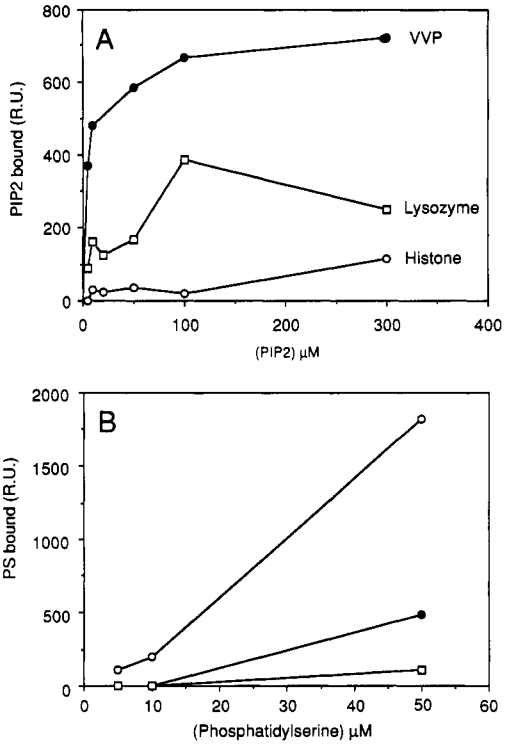

FIGURE 7: Binding of lipids to profilin and control proteins immobilized on BIAcore sensorchips, measured in surface plasmon resonance units (RU's). (A) Dependence of steady-state binding on the concentration of PIP_2 micelles. Proteins on sensorchip: (●) vaccinia profilin; (□) hen egg lysozyme; (○) calf histone. Each point is the average of two experiments. (B) Dependence of steady-state binding on the concentration of PS vesicles. Proteins on sensorchip: (●) vaccinia profilin; (□) hen egg lysozyme; (○) calf histone. Each point is the average of two experiments.

irregular. PIP_2 did not bind to histone immobilized on the sensorchip. Large unilamellar vesicles of 25% PIP_2 with 75% PC (w/w) appeared to bind vaccinia profilin on the same time scale as micelles of pure PIP_2. We were unable to analyze the data quantitatively, because the large vesicles caused an artifactual decrease in the refractive index of the flow chamber buffer, partially cancelling out the surface plasmon resonance signal.

Small sonicated vesicles of PS did not bind to amoeba profilin-II (not shown), but at high concentration interacted weakly with vaccinia profilin (Figure 7B). PS bound to histone but not to lysozyme immobilized on the sensorchip (Figure 7B). Large unilamellar vesicles of 50% (w/w) PC/PS gave no signal on the vaccinia profilin surface (Table 1). None of the lipids tested gave a signal when reacted with a blank sensorchip activated with EDC–NHS without protein present (not shown).

These surface plasmon resonance experiments provided the first data on the kinetics of the interaction of profilin with lipids and put some limits on the values of the rate constants. Since the experiments were done under pseudo-first-order conditions, we fit the time courses of lipid association (Figure 8A) and dissociation (Figure 8B) to single exponentials. Most of the kinetic curves fit exponentials reasonably well considering the geometry of the system. We ascribe the initial lags in the nonideal data to the time required for the diffusion of the 6 nm lipid micelles through the dextran layer containing the immobilized profilin. Association rate constants are all in the range (1–6) $\times$ 10^4 M^{-1} s^{-1}, indicating that binding of lipids to profilin is slow compared to diffusion-limited reactions which have association rate constants of 10^6–10^7 M^{-1} s^{-1}. The

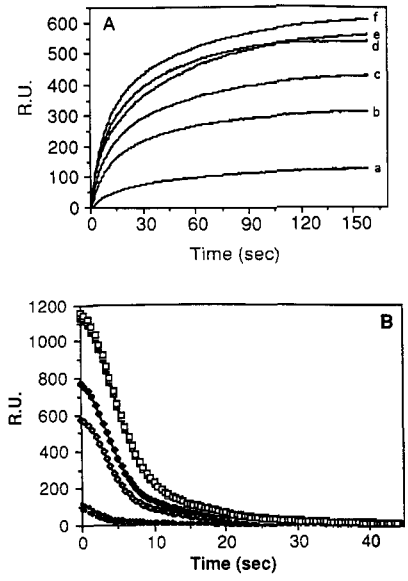

FIGURE 8: Time course of lipid binding and dissociation on profilin biosensor surfaces detected by surface plasmon resonance. (A) PIP_2 micelles binding to vaccinia virus profilin. Various concentrations of micellar PIP_2 flowed through the cell: (a) 1 μM, (b) 5 μM, (c) 10 μM, (d, e) 50 μM, and (f) 100 μM. (B) PIP micelles dissociating from amoeba profilin-II. PIP micelles at concentrations of 20 μM (○, ●), 50 μM (◇, ◆), and 100 μM (□, ■) were bound to the biosensor surface and then dissociated by flow of buffer through the chamber.

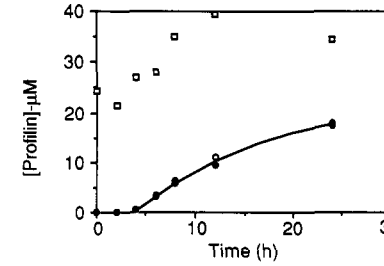

FIGURE 9: Quantitation of vaccinia virus profilin and endogenous HeLa profilin during infection of HeLa cells by vaccinia virus. Vaccinia profilin (circles) and endogenous profilin (squares) were quantitated by immunoblotting at different time points during infection of HeLa cells with 15 pfu/cell vaccinia virus at time zero. Open and closed circles represent scans of different chemiluminescence exposures of the same immunoblot.

association rate constant was calculated assuming that all of the PIP and PIP_2 was in micelles with a molecular mass of 90 kDa. If some of the lipid was in larger particles, the actual association rate constant is larger than we have calculated. Dissociation rate constants are in the range 0.1–0.01 s^{-1} (Table 1). Higher values were generally obtained in the dissociation experiments than by extrapolation of k_{obs} from the association experiments to the y-axis. The dissociation experiments are probably more reliable for estimating the dissociation rate constants.

Equilibrium dissociation constants were calculated from the ratio of the dissociation and association rate constants for amoeba profilin-II and vaccinia profilin binding to PIP and PIP_2. Recombinant amoeba profilin-II binds to PIP_2 micelles with K_d = 3 μM, which is somewhat stronger binding than our previous estimate of 20 μM for native profilin in equilibrium experiments (Machesky et al., 1990). The dissociation equilibrium constant for PIP has not been reported before and is also about 4 μM. Vaccinia profilin has K_d's of 0.2 μM for PIP and 1.3 μM for PIP_2. Thus, by surface plasmon resonance measurements, both vaccinia profilin and amoeba profilin-II bind to PIP and PIP_2 with micromolar affinities, in general agreement with previous studies (Goldschmidt-Clermont et al., 1990; Machesky et al., 1990).

Vaccinia Profilin Is Expressed in HeLa Cells at Micromolar Concentrations during Viral Infection. The synthesis of vaccinia profilin began 4 h after the infection of HeLa cells, and it accumulated to a concentration of 20 μM (Figure 9, circles). This is similar to the concentration of endogenous profilin in these cells (20–40 μM).

Vaccinia Virus Profilin Does Not Complement S. cerevisiae Profilin Null Mutants. Expression of vaccinia profilin did not complement null mutations in the yeast pfy gene. We transformed several strains of *S. cerevisiae* with a recombinant plasmid containing the vaccinia profilin gene (YEpVP) or the vector alone (YEpA). After transformation with YEpVP, five different clones of *S. cerevisiae* carrying a null mutation for yeast profilin (Haarer et al., 1990) expressed viral profilin in concentrations of 7–105 μM, but did not appear to regain a normal phenotype. Expression was quantitated by immunoblotting and scanning densitometry. By light microscopy, the transformed cells were large and rounded, like pfy⁻ yeast containing YEpA (not shown). The growth rates of selected clones (4 and 6) expressing concentrations of vaccinia profilin comparable to the profilin concentrations in HeLa cells were identical to pfy⁻ yeast containing YEpA.

DISCUSSION

The interpretation of our work depends on the assumption that the properties of recombinant vaccinia profilin expressed in *E. coli* are representative of the native protein. We cannot make this comparison directly, since it has not been possible to purify vaccinia profilin from virus-infected cells. However, one of our laboratories has extensively characterized recombinant human and amoeba profilins produced in *E. coli*, without finding any substantial differences with their native counterparts even at atomic resolution [compare Vinson et al. (1993) and Fedorov et al. (1994)]. Recombinant cellular profilins bind to poly(L-proline) and actin like the native profilins (Almo et al., 1994). There is no difference in their enhancement of actin nucleotide exchange or inhibition of actin polymerization. As an additional precaution in the purification of vaccinia profilin, we avoided the urea denaturation and renaturation steps used to purify other profilins. The purified virus profilin has the same Stokes radius as other profilins, so it is not aggregated. Since the recombinant vaccinia profilin binds to lipids much like other profilins, we have assumed that its low affinities for actin and poly(L-proline) are genuine.

Interaction of Vaccinia Profilin with Ligands: Actin, Poly(L-proline), and PIP_2. Vaccinia profilin stands apart from all known profilins in its lower affinity for actin. Although vaccinia profilin can be cross-linked to actin with the zero-length cross-linker EDC, it has no effect on actin polymerization in the concentration range tested. This is not surprising given the the low affinity revealed by the nucleotide exchange assay. Chemical cross-linking must be favorable during the brief encounters of the two proteins. The dissociation equilibrium constant is >35 μM and could be 10–100 times higher. None of the available assays are sensitive in this range, but we can put a lower limit on the K_d from the nucleotide exchange. This experiment also put a lower limit on the dissociation equilibrium constant for the complex of ATP with vaccinia profilin–actin of 0.008 μM, 7-fold weaker than the affinity of ATP for actin alone. Depending on the actual

affinity of vaccinia profilin for actin, the affinity of nucleotide for the complex may be much weaker than 7-fold. Thus, vaccinia profilin enhances nucleotide exchange on actin monomers, but the effect may be much less than 1000-fold enhancement of human platelet profilin (Goldschmidt-Clermont et al., 1991b). This low affinity of vaccinia profilin for actin may explain why the presence or absence of vaccinia profilin expression during infection has no clear effect on actin organization detected by light microscopy (Blasco et al., 1991).

The low affinity of vaccinia profilin for actin is plausibly explained by differences in residues that contact actin in the crystal structure of the complex of bovine profilin and β-actin (Schutt et al., 1993). Vaccinia R115 corresponds to a highly conserved glycine at position 121 in bovine profilin that contacts actin directly. The bulky side chain of R115 would prevent close contact. Similarly, the large side chains of vaccinia Y79 and Y114 (corresponding to bovine profilin E82 and N124) would interfere sterically with binding to actin if the backbone conformation of the two profilins were the same. In addition, vaccinia C66 and G86 will not be able to make electrostatic bonds with actin D286 and D288 like K69 and K90 of bovine profilin. Other factors may also compromise the interaction of vaccinia profilin with actin, but these five differences alone appear to be sufficient to account for the lower affinity of vaccinia profilin.

Similarly, vaccinia profilin lacks several conserved aromatic residues directly implicated in the binding of poly(L-proline) by NMR experiments with amoeba profilin-I (Archer et al., 1994) and human profilin-I (Metzler et al., 1994). A similar poly(L-proline) binding site was predicted for bovine profilin from mutagenesis experiments (Bjorkegren et al., 1993) and the X-ray structure (Schutt et al., 1993). The profilins that bind poly(L-proline) have a tyrosine at the position corresponding to vaccinia profilin isoleucine-6, tryptophan instead of leucine at vaccinia position 31, and histidine or tyrosine instead of arginine at vaccinia position 126. The absence of these three aromatic residues provides a plausible molecular basis for the low affinity of the viral profilin for poly(L-proline).

The PIP_2 binding site on profilins is less well-defined, but comparison of the atomic structures of weakly binding amoeba profilin-I and tightly binding profilin-II by NMR (Vinson et al., 1993) and X-ray crystallography (Fedorov et al., 1994) has identified candidate binding sites involving residues that are largely conserved in vaccinia profilin. The corresponding residues are amoeba profilin-II residues H24, K50, R75, K90, and K93 and vaccinia profilin residues K25, R54, N77, R97, and H99. If arranged in space like these basic residues in amoeba profilin-II, the vaccinia profilin residues will form a pocket with a highly positive electrostatic surface potential suitable for binding PIP and PIP_2.

The slow rate of association of profilins with polyphosphoinositides may be important in signalling reactions as postulated by Goldschmidt-Clermont et al. (1991a). For example, attack of phosphorylated PLC-γ on a cluster of PIP_2 associated with a profilin would presumably release the profilin into the cytoplasm. Slow reassociation would allow considerable hydrolysis of PIP_2 to occur before rebinding of profilin to newly synthesized PIP_2.

Vaccinia Profilin Is Expressed in Host Cells at Concentrations Comparable to Endogenous Cellular Profilin: Possible Implications for Cell Signalling. The concentration of vaccinia virus profilin in infected cells is sufficient to bind a significant fraction of cellular PIP_2. Vaccinia profilin reaches a concentration of 20 μM in infected HeLa cells after 24 h of infection (Figure 9). This value is comparable to the concentration of endogenous HeLa profilin (20–40 μM) before and during a viral infection. These concentrations and the equilibrium constants suggest that most (16–18 μM) of cytoplasmic vaccinia virus profilin would be bound to PIP_2 late during infection of HeLa cells (Table 3). Little vaccinia profilin is expected to bind actin because of its low affinity ($K_d \geq 35$ μM) for actin compared to PIP_2. Obviously, a cell is much more complex than the four-component system modeled in Table 3, since both profilins would also bind PIP and likely other polyphosphoinositides. Nevertheless, this analysis gives us a rough idea of the partitioning of both profilins among their potential ligands. By binding to PIP and PIP_2, vaccinia profilin may compete with or complement the interactions of endogenous profilin with phosphoinositides.

Table 3: Theoretical Calculation of Concentrations of Molecular Species in a Mixture of Physiological Concentrations of HeLa Profilin, Vaccinia Profilin, Thymosin β_4, Unpolymerized Actin, and PIP_2 Based on the Equilibrium Constants for These Interactions[a]

protein	measured or assumed total concn in HeLa cells (μM)	calcd concn[b] (μM) complexed with	
		actin	PIP_2
HeLa profilin	30	0.1–7.4	22–29
vaccinia profilin	20	0.02–2	16.6–18
thymosin β_4	50–400	49–99.6	0
actin	200	100[c]	0

[a] Dissociation equilibrium constants (K_d) were obtained as follows: profilin and PIP_2 (1 μM), Machesky et al., 1990; Goldschmidt-Clermont et al., 1990; profilin and actin (3 μM), Goldschmidt-Clermont et al., 1991b; viral profilin and actin (30 μM), this paper; viral profilin and PIP_2 (3.6 μM), this paper; thymosin β_4 and actin (1 μM), Yu et al., 1993. [b] Concentrations are given in ranges because we estimated the thymosin β_4 content of HeLa cells to be between 50 and 400 μM, based on personal communications with Pascal Goldschmidt-Clermont and Vivianne Nachmias. Concentrations of other species were obtained from the following sources: profilin, viral profilin; this paper. [c] Concentration of polymerized actin in the cell.

Why Would a Virus Have a Functional Profilin Gene? Although vaccinia profilin is not required for viral replication in tissue culture (Blasco et al., 1991) it is unlikely that the virus would maintain and express a gene encoding profilin unless the protein confers some advantage upon the virus. One role may be in modulating autostimulation by a growth factor expressed by the virus. Vaccinia virus growth factor (Blomquist et al., 1984; Brown et al., 1985; Reisner, 1985) is a mitogen related to EGF by amino acid sequence and receptor binding properties (Gregory, 1975). Purified VGF competes with EGF, when applied to A431 human epidermal carcinoma cells (Stroobant et al., 1985; Twardzik et al., 1985). VGF stimulates tyrosine phosphorylation of EGF receptors to the same degree as purified EGF (King et al., 1986). VGF is released from infected cells early during infection and may stimulate the proliferation of neighboring cells, thereby enhancing virus spread (Buller et al., 1988). Expression of vaccinia profilin might regulate the response of infected cells to VGF. For example, infection with VGF null virus inhibits ATP-induced PI turnover but not basal levels of PI turnover (Oliver et al., 1992). Viral infection inhibited both G-protein-dependent and -independent pathways of PLC activation. Except for slightly higher levels of PIP_2, inositol phospholipids levels were unaffected. The authors concluded that vaccinia virions express at least one molecule capable of inhibiting PLC activity. Although expression of viral profilin is not required to inhibit G-protein-dependent PLC activity (data not shown), these investigators argued that profilin and other viral proteins may be PLC inhibitors, because each of the several PLC isoforms has unique regulatory mechanisms. This

is consistent with evidence that profilin inhibits PLC-γ but not PLC-β (Goldschmidt-Clermont et al., 1990). Biochemical studies will be required to clarify these mechanisms.

Tight Binding to PIP_2 Is Not Sufficient for Normal Profilin Function in Vivo. Expression of micromolar quantities of vaccinia profilin in *S. cerevisiae* profilin null cells did not complement profilin null mutants. Yeast profilin null cells display a variety of characteristics suggestive of defective actin cytoskeleton function (Haarer et al., 1990). Actin localization is abnormal, (bar structures in cytoplasm), chitin localization is abnormal and cells are larger than normal, all of which occur in actin mutants. It is proposed that actin mutations affect chitin deposition, because actin is needed for polarized secretion in actively growing cells (Shortle et al., 1984; Novick & Botstein, 1985; Novick et al., 1989). Further evidence that profilin affects the actin cytoskeleton *in vivo* is that overexpression of profilin in *S. cerevisiae* will suppress mutant phenotypes caused by actin overexpression (Magdolen et al., 1993).

The failure of vaccinia profilin to complement yeast profilin null mutants is evidence that the actin binding and/or poly(L-proline) binding activities of profilin are important *in vivo*. Since the transformed cells express concentrations of vaccinia profilin up to 105 μM, the failure to complement is most likely due to some quality of the vaccinia profilin that is different from endogenous profilin. Since poly(L-proline) binding is not essential for the function of yeast profilin (Haarer et al., 1993), the lack of actin binding may be the responsible defect in vaccinia profilin. In contrast, both profilin-I and profilin-II from *Acanthamoeba* will complement yeast profilin null mutants (Vojtek et al., 1991). These isoforms are indistinguishable with respect to actin binding, nucleotide exchange, polymerization inhibition, and poly(L-proline) binding (Kaiser et al., 1986; Machesky, unpublished observations), but profilin-II binds to PIP_2 with a K_d of $\sim$2–10 μM, while profilin-I binds very weakly ($K_d \sim$ 100–500 μM).

Although vaccinia profilin and cellular profilins differ in their affinity for actin, we do not yet know if the consequences of their binding to PIP_2 and PIP are identical. Vaccinia profilin may have a different effect on PI turnover than cellular profilin. A better understanding of the role of vaccinia profilin–PIP_2 interactions and also of the physiological relevance of profilin binding to poly(L-proline) will elucidate whether actin binding alone is essential for profilin function *in vivo*.

ACKNOWLEDGMENT

We thank Robert Jensen for guidance on the yeast experiments, Pascal Goldschmidt-Clermont for critical reading of the manuscript, and Michael Robinson of Pharmacia Biosensor and Terry Prospero of the MRC Laboratory of Molecular Biology for assistance with BIAcore experiments.

REFERENCES

Almo, S., Pollard, T. D., Way, M., & Lattman, E. E. (1994) *J. Mol. Biol. 236*, 950–952.

Ampe, C., Vandekerckhove, J., Brenner, S. L., Tobacman, L., & Korn, E. D. (1985) *J. Biol. Chem. 260*, 834–840.

Ampe, C., Sato, M. Pollard, T. D., & Vandekerckhove, J. (1988) *Eur. J. Biochem. 170*, 597–601.

Archer, S., Vinson, V., Pollard, T. D., & Torchia, D. (1994) *FEBS Lett. 337*, 145–151.

Barshop, B. A., Wrenn, R. F., & Frieden, C. (1983) *Anal. Biochem. 130*, 134–145.

Bjorkegren, C., Rozycki, M., Schutt , C. E., Lindberg, U., & Karlsson, R. (1993) *FEBS Lett. 333*, 123–126.

Blasco, R., Cole, N. B., & Moss, B. (1991) *J. Virol. 65*, 4598–4608.

Blomquist, M. C., Hunt, L. T., & Barker,W. C. (1984) *Proc. Natl. Acad. Sci. U.S.A. 81*, 7363–7367.

Brown, J. P., Twardzik, D. R., Marquardt, H., & Todaro, G. J. (1985) *Nature 313*, 491–492.

Buller, R. M. L., Chakrabarti, S., Moss, B., & Fredrickson, T. (1988) *Virology 164*, 182–192.

Cooley, L., Verheyen, E., & Ayers, K. (1992) *Cell 69*, 173–184.

Drobak, B. K. (1993) *Plant Physiol. 102*, 705–709.

Edmatsu, M., Hirono, M., & Watanabe, Y. (1990) *Biochem. Biophys. Res. Commun. 170*, 957–962.

Fagerstam, L. G., Frostell-Karlsson, A., Karlsson, R., Persson, B., & Ronnberg, I. (1992) *J. Chromatogr. 597*, 397–410.

Fedorov, A. A., Magnus, K. A., Graupe, H., Lattman, E. E., Pollard, T. D., & Almo, S. C. (1994) *Proc. Natl. Acad. Sci. U.S.A.* (in press).

Goldschmidt-Clermont, P. J., Machesky, L. M., Baldessare, J. J., & Pollard,T. D. (1990) *Science 247*, 1575–1576.

Goldschmidt-Clermont, P. J., Kim, J. W., Machesky, L. M., Rhee, S. G., & Pollard, T.D. (1991a) *Science 251*, 1231–1233.

Goldschmidt-Clermont, P. J., Machesky, L. M., Doberstein, S. K., & Pollard, T. D. (1991b) *J. Cell Biol. 113*, 1081–1089.

Gregory, H. (1975) *Nature 257*, 325–327.

Haarer, B. K., Lillie, S. H., Adams, A. E. M., Magdolen, V., Bandlow, W., & Brown, S. S. (1990) *J. Cell Biol. 110*, 105–114.

Haarer, B. K., Petzold, A. S., & Brown, S. S. (1993) *Mol. Cell Biol. 13*, 7864–7873.

Haugwitz, M., Noegel, A. A., Rieger, D., Lottspeich, F., & Schleicher, M. (1991) *J. Cell Sci. 100*, 481–489.

Hendrickson, H. S. (1969) *Ann. N.Y. Acad. Sci. 165*, 668–676.

Hitzeman, R. A., Leung, D., Perry, J., Kohr, W. J., Levine, H. L., & Goeddel, D. V. (1983) *Science 219*, 620–625.

Honore, B., Madsen, P., Andersen, A. H., & Leffers, H. (1993) *FEBS Lett. 330*, 151–155.

Kaiser, D. A., Sato, M., Ebert, R. F., & Pollard, T. D. (1986) *J. Cell Biol. 102*, 221–226.

Kaiser, D. A., Goldschmidt-Clermont, P. J., Levine, B. A., & Pollard, T. D. (1989). *Cell Motil. Cytoskeleton 14*, 251–262.

King, C. S., Cooper, J. A., Moss, B., & Twardzik, D. R. (1986) *Mol. Cell. Biol. 6*, 332–336.

Kwiatkowski, D. J., & Bruns, C. A. (1988) *J. Biol. Chem. 261*, 88–91.

Laemmli, U. K (1970) *Nature (London) 227*, 680–685.

Lal, A. A., & Korn, E. D. (1985) *J. Biol. Chem. 260*, 10132–10138.

Lassing, I., & Lindberg, U. (1985) *Nature 318*, 472–474.

Lassing, I., & Lindberg, U. (1988) *J. Cell Biochem. 37*, 255–268.

Machesky, L. M., Goldschmidt-Clermont, P. J., & Pollard, T. D. (1990) *Cell Regul. 1*, 937–950.

Magdolen, V., Drubin, D., Mages, G., & Bandlow, W. (1993) *FEBS Lett. 316*, 41–47.

Maniatis, T., Fritsch, E. F., & Sambrook, J. (1982) *Molecular Cloning: A Laboratory Manual*, Cold Spring Harbor Laboratory, Cold Spring Harbor, NY.

Metzler, W. J., Constantine, K. L., Friedrichs, M. S., Bell, A. J., Ernst, E. G., Lavoie, T. B., & Mueller, L. (1993) *Biochemistry 32*, 13818–13829.

Metzler, W. J., Bell, A. J., Ernst, E., Lavoie, T. B., & Mueller, L. (1994) *J. Biol. Chem. 269*, 4620–4625.

Mockrin, S. C., & Korn, E. D. (1980) *Biochemistry 19*, 5359–5362.

Nishida, E. (1985) *Biochemistry 24*, 1160–1164.

Novick, P., & Botstein, D. (1985) *Cell 40*, 405–416.

Novick, P., Osmond, B. C., & Botstein, D.(1989) *Genetics 121*, 659–674.

Nowak, E., & Goody, R. S. (1988) *Biochemistry 27*, 8613–8617.

Nystrom, L. E., Lindberg, U., Kendrick-Jones, J., & Jakes, R. (1979) *FEBS Lett. 101*, 161–165.

Oeschner, U., Magdolen, V., & Bandlow, W. (1987) *Nucleic Acids Res. 15*, 9078.
Oliver, K. G., Buller, M. L., Hughes, P. J., Putney, J. W., & Palumbo, G. J. (1992) *J. Biol. Chem. 267*, 25098–25103.
Pantaloni, D., & Carlier, M.-F. (1993) *Cell 75*, 1007–1014.
Pollard, T. D., & Cooper, J. A. (1984) *Biochemistry 23*, 6631–6641.
Pollard, T. D., & Rimm., D. L. (1990) *Cell Motil. Cytoskeleton* 20, 169–177.
Pollard, T. D., Goldberg, I., & Schwarz, W. (1992) *J. Biol. Chem. 267*, 20339–20345.
Reisner, A. H. (1985) *Nature 313*, 801–803.
Rosenberg, A. H., Lade, B. D., Chui, D.-S., Lin, S.-W., Dunn, J. J., & Studier, F. W. (1987) *Gene 56*, 125–135.
Schutt, C., Myslik, J. C., Rozychi, M. D., Goonesekere, N. C. W., & Lindberg, U. (1993) *Nature 365*, 810–816.
Sherman, F., Fink, G. R., & Hicks, J. B. (1982) *Laboratory Course Manual for Methods in Yeast Genetics*, Cold Spring Harbor Laboratory, Cold Spring Harbor, NY.
Shortle, D., Novick, P., & Botstein, D. (1984) *Proc. Natl. Acad. Sci. U.S.A. 81*, 4889–4893.
Spudich, J. A., & Watt, S. (1971) *J. Biol. Chem. 246*, 4866–4871.
Sri Widada, J. S., Ferraz, C., & Liautard., J. P. (1989) *Nucleic Acids Res. 17*, 2855.
Stroobant, P., Rice, A. P., Gullick, W. J., Cheng, D. J., Kerr, I. M., & Waterfield, M. D. (1985) *Cell 42*, 383–393.
Studier, F. W., Rosenberg, A. H., Dunn, J. J., & Dubendorf, J. W. (1990) *Methods Enzymol. 185*, 60–89.
Sugiura, Y. (1981) *Biochim. Biophys. Acta 641*, 148–159.
Takagi, T., Mabuchi, I., Hosoya, H., Furuhashi, K., & Hatano, S. (1991) [Published erratum (1991) *Eur. J. Biochem. 197*, 819] *Eur. J. Biochem. 192*, 777–781.
Twardzik, D. R., Brown, J. P., Ranchalid, J. E., Todaro, G. J., & Moss, B. (1985) *Proc. Natl. Acad. Sci. U.S.A. 82*, 5300–5304.
Valenta, R., Duchene, M., Pettenburger, K., Sillaber, C., Valent, P., Breitenbach, M., Rumpold, H., Kraft, D., & Schellner, O. (1991) *Science 109*, 619–626.
Vallier, P., DeChamp, C., Valenta, R., Vial, O., & Deviller, P. (1992) *Clin. Exp. Allergy 22*, 774–782.
Vandekerckhove, J. S., Kaiser, D. A., & Pollard, T. D. (1989) *J. Cell Biol. 109*, 619–626.
Vinson, V., Archer, S., Lattman, E. E., Pollard, T. D., & Torchia, D. (1993) *J. Cell Biol. 122*, 1277–1283.
Vojtek, A., Haarer, B., Field, J., Gerst, J., Pollard, T. D., Brown, S., & Wigler, M. (1991) *Cell 66*, 497–505.
Wachsstock, D. H., & Pollard, T. D. (1994) *Biophys. J.* (in press).
Waechter, F., & Engel, J. (1975) *Eur. J. Biochem. 57*, 453–459.
Yu, F.-X., Lin, S.-C., Morrison-Bogorad, M., Atkinson, M. A. L., & Yin, H. L. (1993) *J. Biol. Chem. 268*, 502–509.